The NASA Dryden AAR Project: A Flight Test Approach to an Aerial Refueling System

Jennifer L. Hansen,* James E. Murray,† and Norma V. Campos‡
NASA Dryden Flight Research Center, Edwards, California, 93523

The integration of uninhabited aerial vehicles (UAVs) into controlled airspace has generated a new era of autonomous technologies and challenges. Autonomous aerial refueling would enable UAVs to travel further distances and loiter for extended periods over time-critical targets. The NASA Dryden Flight Research Center recently has completed a flight research project directed at developing a dynamic hose and drogue system model to support the development of an automated aerial refueling system. A systematic dynamic model of the hose and drogue system would include the effects of various influences on the system, such as flight condition, hose and drogue type, tanker type and weight, receiver type, and tanker and receiver maneuvering. Using two NASA F/A-18 aircraft and a conventional hose and drogue aerial refueling store from the Navy, NASA has obtained flight research data that document the response of the hose and drogue system to these effects. Preliminary results, salient trends, and important lessons are presented.

Nomenclature

AAR	=	automated aerial refueling
AFF	=	autonomous formation flight
AOA	=	angle of attack, deg
AOI	=	area of influence
ARS	=	aerial refueling store
DDVP	=	dimensionless drogue vertical position, $\frac{V_D}{L_H}$
g	=	gravitational acceleration
GPS	=	global positioning system
ILS	=	instrument landing system
KIAS	=	knots indicated airspeed
L_H	=	straight-line distance from hose exit point to hose and drogue coupling, ft
MCR	=	mission control room
MSL	=	mean sea level
NASA	=	National Aeronautics and Space Administration
Pos	=	position
T/N	=	tail number
UAV	=	uninhabited aerial vehicle
V_D	=	altitude difference between hose and drogue coupling and hose exit point, ft

I. Introduction

The integration of a new class of unmanned airplanes into controlled airspace has created new challenges and technological hurdles. The technology required for reliable uninhabited aerial vehicle (UAV) deployment just recently became accessible, although the use of UAVs dates back to the 1800s.[1] The UAVs have had a broad impact on the aerospace and defense industries partly because of recent rapid development and increase in accessibility of

* Aerospace Engineer, Aerodynamics Branch, P.O. Box 273/Mail Stop D-2228, AIAA Member.
† Aerospace Engineer, Aerodynamics Branch, P.O. Box 273/Mail Stop D-2228.
‡ Engineering Student, Aerodynamics Branch, P.O. Box 273/Mail Stop D-4840, AIAA Student Member.

several enabling technologies, such as global positioning systems (GPSs), microelectronic mechanical systems (MEMS), lightweight composites, and so forth. Today's operational UAVs have significant sensing, receiving, and relaying capabilities, and can loiter at altitudes up to 60,000 ft for durations of more than 24 hours. They are inexpensive enough to manufacture in large quantities and dependable enough to use for mission-critical tasks. Several types of UAVs have been successfully demonstrated in wartime during the last two decades, and as a result, demand for them is increasing.

An obvious benefit of UAVs is the elimination of human presence and risk to the pilot. Despite extensive autonomous capabilities of UAVs, a pilot in the cockpit cannot be replaced. Many routine pilot tasks, such as aerial refueling, become significantly more difficult when performed autonomously. Automated aerial refueling has never been demonstrated in flight, and this capability would greatly benefit the UAV community. To aid this development effort, NASA Dryden Flight Research Center (Edwards, California) initiated the Automated Aerial Refueling (AAR) project to acquire flight data on hose and drogue system dynamics, correlate results with an analytical model of the hose and drogue system, and develop a validated model for designing automated aerial refueling control systems. Figures 1 (EC03-0293-04) and 2 (EC03-0293-06) show the two aircraft from the AAR project in the full test configuration. (All photographs appearing in this report are courtesy of the NASA Dryden Flight Research Center Imaging Department.)

Figure 1. In-flight AAR configuration.

Figure 2. Bottom view of in-flight AAR configuration.

II. The AAR Project

The AAR project evolved from the Autonomous Formation Flight (AFF) project. From June 2000 to December 2001, the AFF project, using relative-position station-keeping technology between two airplanes, demonstrated the possible fuel savings of formation flight.[2] Modified slightly, these GPS-based technologies and airborne telemetry systems from the AFF project were used in the AAR project to monitor relative position and velocity in real time and provide guidance to the pilots in flying the test points.[3] The AAR project used the same airplanes, simulation environment, pilots, technicians, and engineers as those used in the AFF project.

A. Project Objective

The primary objective for the NASA Dryden AAR project was to deliver a flight-validated dynamic hose and drogue system model to support the development of an automated aerial refueling system. This objective would be supported with a simulation created from an in-house, boom-type refueling simulation, which used elements from the simulation technology developed during the AFF program.

B. Flight Test Approach

The first series of AAR project flights focused on clearing a NASA F/A-18A aircraft (McDonnell Douglas Corporation, St. Louis, Missouri) to carry the aerial refueling store (ARS). After the ARS captive carry envelope of the tanker was cleared, the flight test envelope was expanded based on ARS functionality and hose and drogue system response. The envelope was defined by the flight conditions in which the hose and drogue system exhibited acceptable extension and retraction characteristics and acceptable responses during engagements. The tanker clearance flights are discussed in detail in section III, "Tanker Clearance Flight Tests."

The next step in obtaining flight data for validation of the hose and drogue system model was to perform the flight research tests. The research maneuvers were designed to isolate the change in drogue position as a function of individual influences, such as flight condition, hose and drogue type, tanker type and weight, receiver type, and tanker and receiver maneuvering. Various receiver influences on the drogue were investigated, such as closing direction, closing speed, and weight. The hose and drogue system model is discussed in detail in the next section, "Hose and Drogue System Model."

C. Hose and Drogue System Model

The proposed dynamic model would predict hose and drogue positions as a function of flight condition, drogue condition, hose weight effects, tanker effects, and receiver effects. The position of the drogue relative to the tanker was hypothesized to be a function of several independent variables and could be decomposed into the superposition of the constituent effects,

$$\Delta Pos = \Delta Pos_{FltCond} + \Delta Pos_{Drogue} + \Delta Pos_{Hose} + \Delta Pos_{Tanker} + \Delta Pos_{Receiver} \quad (1)$$

The independent variables are divided into several categories. Flight condition effects include those imposed by airspeed and altitude. Drogue effects include the effects from a new drogue as opposed to an old drogue, or a high-drag drogue as opposed to a low-drag drogue. Hose effects are based on whether the hose is empty or full. Tanker effects consist of tanker weight, configuration, and type of downwash field (type of tanker). Receiver effects consist of closing direction, closing velocity, and upwash field (type of receiver). A hose and drogue system model was postulated to be defined by the superposition of these effects, and the flight data was obtained to address that postulation. Regardless, an automated aerial refueling controller must be robust enough to work at numerous flight conditions and with various receivers. The first step towards this effort was to find a representative aircraft and refueling store configuration and define the operational flight envelope.

III. Tanker Clearance Flight Tests

The ARS, originally developed for use on an S-3 aircraft, had been cleared on an F/A-18 E/F airplane known as the Super Hornet (Boeing Company, St. Louis, Missouri).[4] The Super Hornet is larger and more capable than previous Hornet models. NASA Dryden has several of the previous model F/A-18 airplanes, two of which supported the AFF project. The earlier model F/A-18A airplane had to be cleared to fly the S-3 ARS before any research flights could be conducted.

A. Test Aircraft Description

The F/A-18 aircraft is a supersonic, high-performance fighter with a digital flight control system. The tanker airplane that carried the ARS, NASA aircraft tail number (T/N) 847, is a single-seat F/A-18A airplane (Fig. 3) (EC03-0298-06). The receiver airplane, NASA aircraft T/N 845, is a two-seat, preproduction F/A-18 airplane that has been extensively modified to conduct specialized flight systems research (Fig. 4) (EC03-0298-09).

Figure 3. NASA aircraft T/N 847 (tanker).

Figure 4. NASA aircraft T/N 845 (receiver).

B. F/A-18A Airplane ARS Captive Carry Envelope Expansion

A 4-in. adapter designed for fuel tanks was successfully integrated with the F/A-18A airplane to attach the ARS to the centerline with adequate landing gear clearance. A thorough tanker envelope expansion with adapter and ARS installed was performed to assess handling qualities and landing gear operation, and to verify structural analysis. Maneuvers included landing gear extensions and retractions, touch-and-go landings, doublets, steady-heading sideslips, push-over-pull-ups, and bank-to-bank rolls in both a power approach and nominal configuration. As a result, NASA aircraft T/N 847 was cleared to carry the ARS to altitudes of 30,000 ft and Mach numbers to 0.8 (Fig. 5).

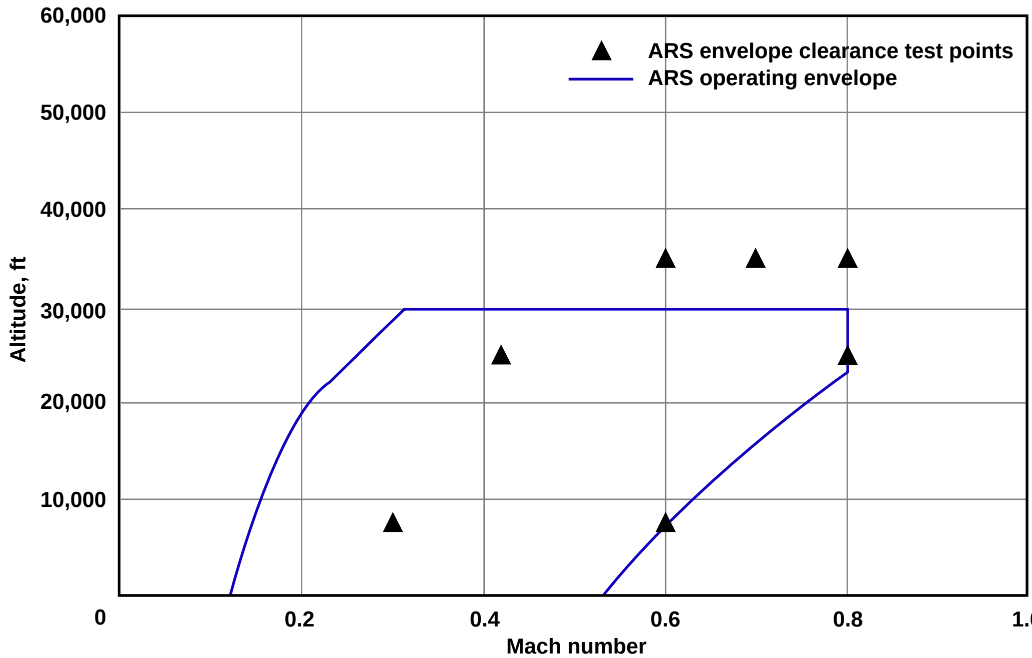

Figure 5. NASA aircraft T/N 847 tanker ARS captive carry envelope.

C. ARS Operational Envelope Expansion

Before active flight testing could begin, definition of the ARS operational envelope was necessary. The ARS envelope expansion had four objectives: (1) verify the hose and drogue extension and retraction test conditions, (2) verify engagement airspeeds and demonstrate successful engagement, (3) identify any hose instabilities that might exist, and (4) verify and update tanker-specific procedures. The ARS uses dynamic pressure to power the hydraulics, which control the hose (Fig. 6). A ram air turbine (RAT) is located on the nose of the ARS, and once activated, it spins and drives the hydraulic pump responsible for hose extension and retraction. The operational envelope was defined by three conditions: no contact between the drogue and tanker on extension or retraction, sufficient hydraulic power for hose retraction, and acceptable receiver engagement performance.

At high airspeeds, the drogue position was close to the tanker and retracted quickly, resulting in occasional drogue contact along the aft midline of the tanker aircraft. The upper limit of the airspeed envelope for retraction was defined to prevent contact. At low airspeeds, the RAT spun too slowly or stopped, resulting in insufficient ARS hydraulic pressure to retract or extend the hose. This condition defined the lower limit of the airspeed envelope for retractions and extensions. Extensions were cleared for altitudes ranging from 7,500 to 30,000 ft and airspeeds ranging from 175 to 250 KIAS. Retractions were explored over the same region, but the upper airspeed was limited to 210 KIAS because of potential contact between the drogue and tanker. Engagements were cleared over the same altitudes, but airspeed limits ranged from 175 to 280 KIAS, depending on altitude (Table 1).

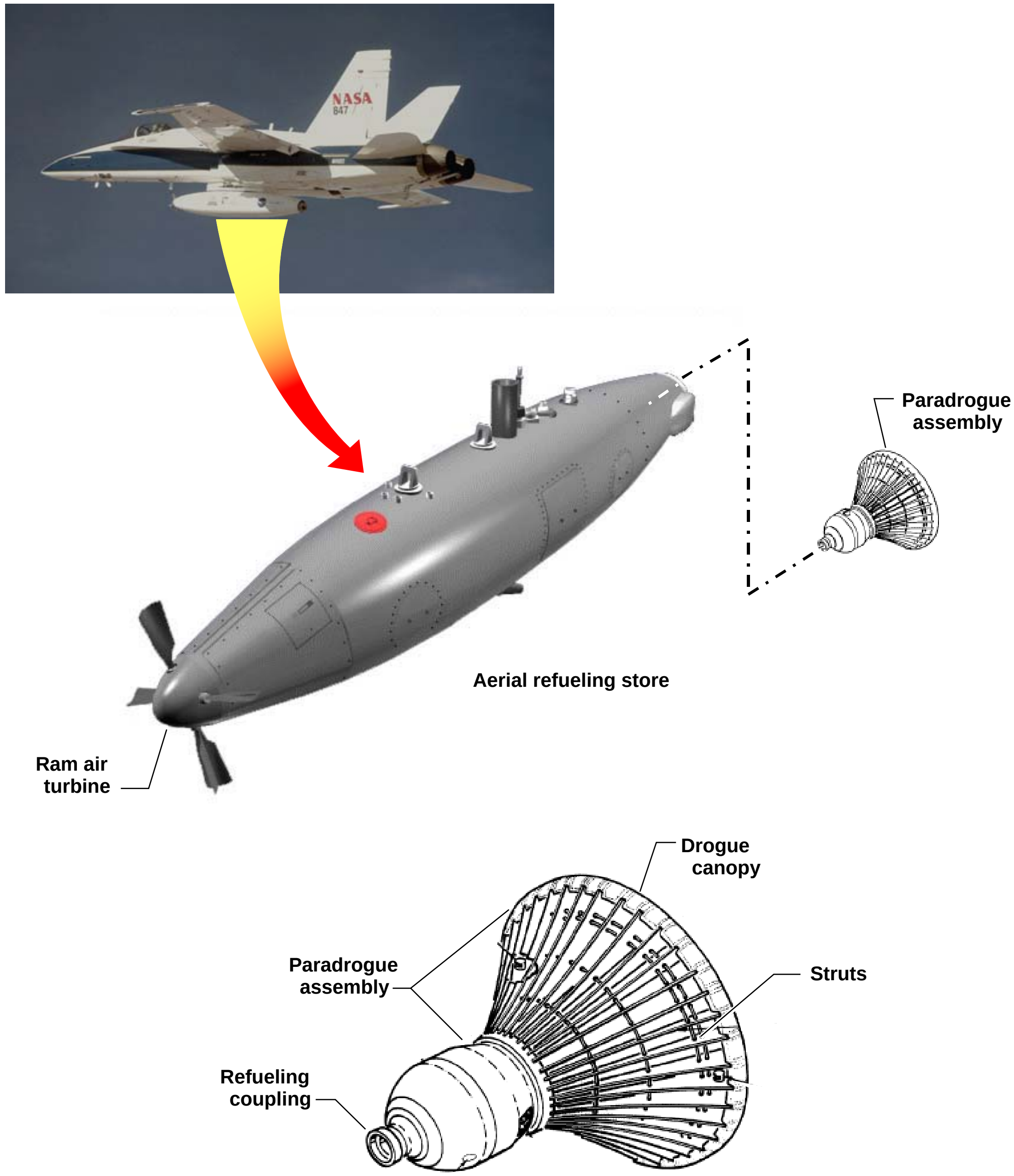

Figure 6. ARS assembly and installation on the F/A-18A airplane.

Table 1. ARS operational limits.

Condition		Limitation
Altitude		7,500 to 30,000 ft MSL
Power On (RAT unfeathered)		175 to 300 KIAS / 0.80 indicated Mach number
Hose Extension		175 to 250 KIAS
Hose Extended		175 to 300 KIAS / 0.80 indicated Mach number
Drogue/Probe Engagement and Transfer	7,500 ft MSL	175 to 250 KIAS
	30,000 ft MSL	185 to 280 KIAS
Hose Retraction		175 to 210 KIAS
Fuel Jettison		Not Authorized
Hose Jettison		250 KIAS / 1 *g* level
Pitch		±5°
Roll		±30°
Yaw		Balanced Flight

D. Qualitative Assessment of Hose and Drogue Position

The next step during the tanker clearance flight tests was to perform an initial qualitative assessment of the free-stream hose and drogue position and dynamic response. For these initial flights, neither aircraft was configured with the video-based measurement equipment. Hose and drogue positions were monitored using an uncalibrated, hand-held video system in the back seat of a chase aircraft. Steady-state hose and drogue positions were recorded during straight-and-level flight to obtain the approximate change in position with flight condition. Stabilized cruise data were acquired with and without the hose and drogue system extended. In-flight, real-time drag measurements of the hose and drogue system were performed by means of AFF-refined drag calculation methods.[5] This test was the first in which hose and drogue system drag was measured through the use of an in-flight thrust measurement technique. These data were analyzed postflight, and the qualitative results were used to guide the flight test plan for the next phase of research flights.

IV. Drogue Mapping Flight Tests

Validation of the hose and drogue system model requires accurate measurements of relative positions and rates of the hose and drogue, in addition to those of the two aircraft. Incremental development and validation of the model require sufficient isolation of the individual influences on the hose and drogue system so that the effects of each influence can be accurately gauged. To address these concerns, several heritage systems were used to provide guidance information to the pilots; two fully instrumented research airplanes were used for the flight test; a videogrammetric camera system was installed on both aircraft to accurately measure the movement of the hose and drogue; and flight test maneuvers were specifically tailored to sufficiently isolate each influence. The remainder of this section describes these systems and maneuvers in detail.

A. AFF Heritage

A distinctive achievement of the AFF project was accurate real-time relative-position station keeping, which was enabled through GPS-based and airborne telemetry systems.[3] These systems enabled the pilot to use switches in the cockpit to select a preprogrammed position relative to the other aircraft and use the instrument landing system (ILS) needles to maintain that position. These systems enabled the pilot to manually fly very accurate relative positions, which enhanced the quality of the force and moment data.[6] For the AAR project, these same systems enabled the pilot to fly a fine grid of test points near the drogue, generally within ±2 ft in real time.

B. AAR Reference System

Figure 7 shows the reference system used in this report. The position of the receiver was defined as the location of its GPS antenna relative to the GPS antenna of the tanker. Each antenna was located just forward of the canopy on the nose of each airplane, close to the centerline. Most of the test points that the receiver flew were at a relative longitudinal position that placed the tip of the probe in the *y*-*z* plane of the drogue canopy.

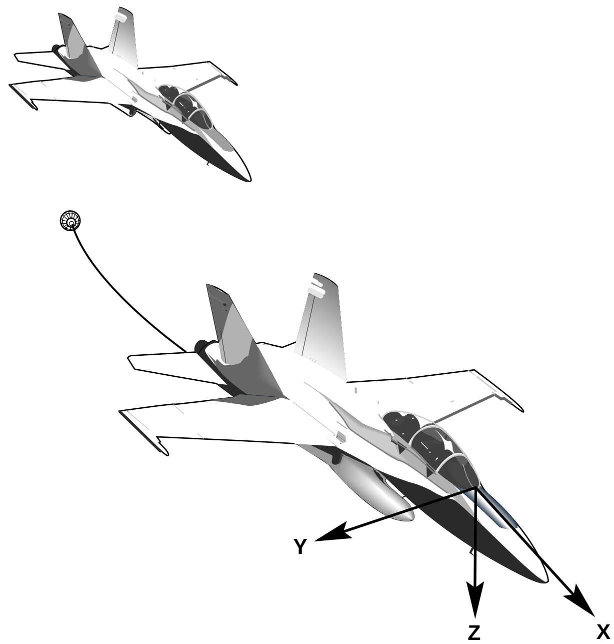

Figure 7. AAR reference system.

C. Drogue-Tracking Options

Two approaches to in-flight measurement of the hose and drogue position were considered. The first approach involved installing a GPS antenna on the drogue. Such an installation would provide accurate time-correlated drogue position measurements that could be postflight processed to within ±6 in. This approach has many disadvantages, particularly the risk associated with a powered GPS antenna attached to the hose and drogue system. Powering an antenna on the drogue requires either a battery located on the drogue or a power cord in the fuel-filled hose. The extra mass of a battery and/or antenna on the drogue might alter the hose and drogue system response. Installing a GPS unit on the drogue requires a significant number of additional clearance flights to ensure that the unit could endure repeated refueling engagements. In addition to introducing integration and safety issues, a GPS unit on the drogue would provide only one measurement, and only when the antenna is able to receive GPS satellite signals. Because of these issues, this approach was deemed too expensive and time-consuming for the low data return and scope of the project.

The second approach involved the use of multiple video cameras mounted to the aircraft to measure the hose and drogue position. This approach ultimately was judged more feasible and effective than installing a GPS unit on the drogue. The objective of the video-based imaging system was to measure the position of multiple points on the hose and drogue system at a sample rate sufficient to capture all the important dynamic modes, and with sufficient accuracy and precision such that the measurements could be used as model validation data. The approach used two pairs (one pair on each test aircraft) of time-synchronized video cameras to image the hose and drogue system in flight. In postflight processing, the pixel coordinates of selected target points on the hose and drogue system were extracted from the video record for each camera station, and the 3-D coordinates (in the aircraft reference frame) of each target point were calculated by a triangulation algorithm. This approach had the advantage of eliminating impact on the hose and drogue system and reducing impact to the airplanes. Furthermore, the hardware was readily available and inexpensive. Although the quantitative position data were not available in real time, one channel of video from each aircraft could be selected by the flight crew for transmission to the mission control room (MCR), where hose and drogue movement could be monitored.

D. Video System Description

The video-based measurement system consisted of two cameras on each aircraft. The cameras on the tanker aircraft were installed facing aft at nominally symmetric locations at the trailing edge of the outboard wing pylons (Fig. 8). The cameras imaged the region aft and below the tanker where the hose and drogue system was expected to deploy in flight. The cameras on the receiver aircraft were installed facing forward on the right side. One camera was located on the wingtip missile rail, and the other was located on the forward edge of the inboard wing pylon (Fig. 9). The cameras imaged the region in the vicinity of the refueling probe along the right side of the aircraft and forward of the canopy, where the drogue was expected to be located during refueling engagements. The head-up display (HUD) camera on the receiver aircraft also provided useful qualitative imagery during the research program.

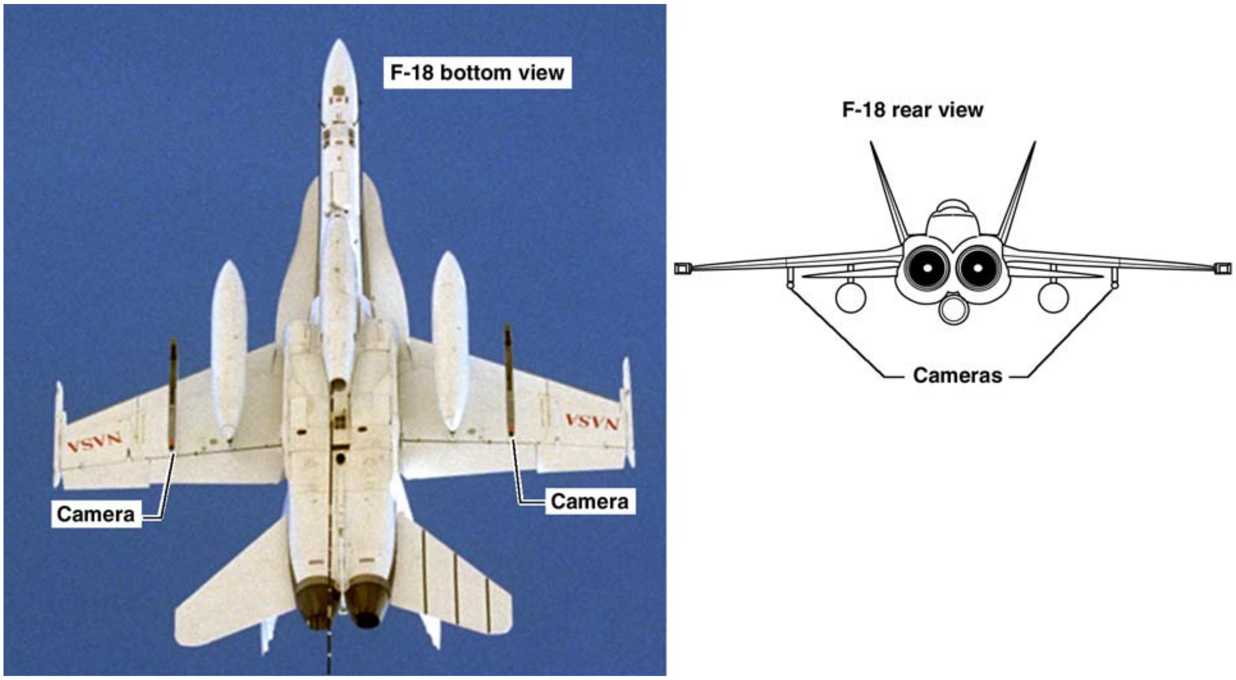

Figure 8. NASA aircraft T/N 847 (tanker cameras).

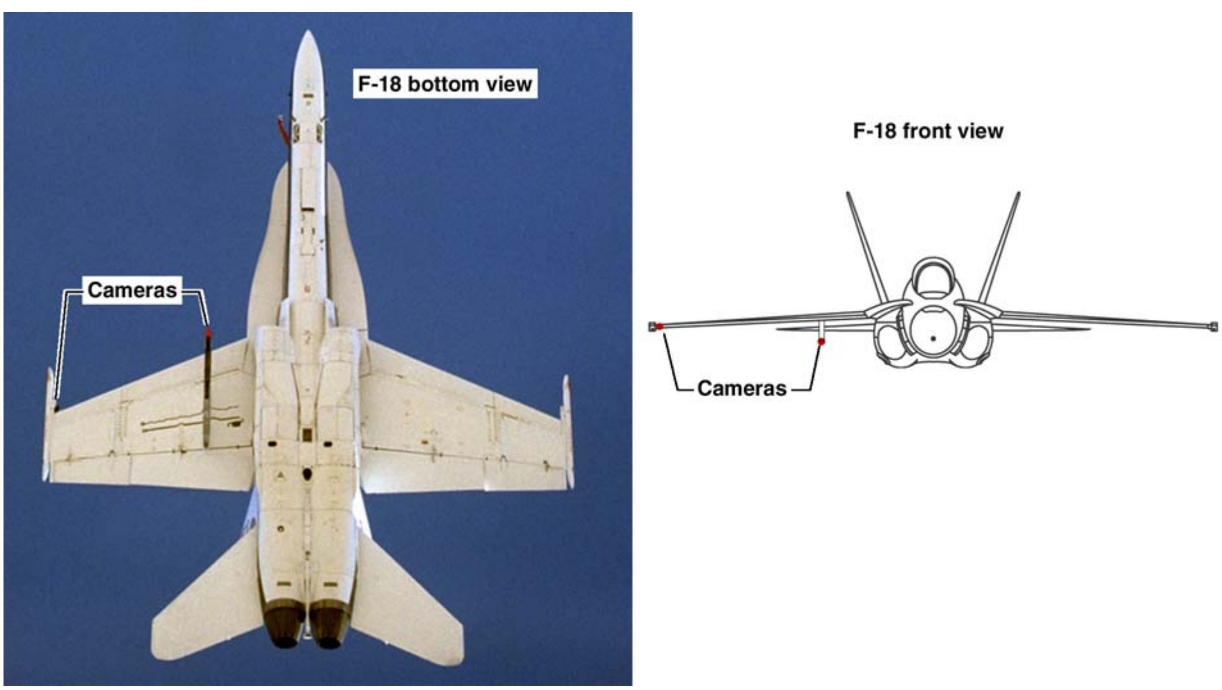

Figure 9. NASA aircraft T/N 845 (receiver cameras).

The GPS date and time were digitally overlayed on the video imagery for each camera, and each video camera was secured in a custom 3-axis (pitch, roll, yaw) mount inside an unpressurized enclosure with optical glass window. Each video camera was only roughly aimed to the expected location of the drogue in flight and then securely locked in position. Postinstallation calibration techniques were used to experimentally identify the alignment of each camera instead of precision-aligning each camera with respect to the aircraft.

To facilitate data recording, each aircraft was fitted with a three-channel videotape recorder (called the triple-deck recorder), which recorded signals from the two wing-mounted cameras and the HUD camera signal. To monitor the hose and drogue system in flight from the MCR, each aircraft was able to transmit one channel to the ground. The flight crew used a three-position switch in the cockpit to select which of the three camera views was transmitted to the MCR.

To maximize data return, the location of multiple target points on the hose, drogue, and both aircraft were measured during each flight test maneuver. To accomplish this task, several superficial enhancements were made to the aircraft and hose and drogue system. Several prominent features on each aircraft, visible in the video images, were identified as additional target points. Some of these points were enhanced with high-contrast markings (for example, white "X" marks made with tape) to aid in measurement. Existing stripes on the black hose were rejuvenated with fresh white paint, and additional white stripes were painted every 2 ft along the hose. The drogue assembly was repainted to reduce glare, improve contrast, and better identify and localize the connection point between the hose and drogue. The rigid forebody of the drogue assembly was painted with a colored roll pattern to identify roll angle changes during flight maneuvers.

E. Video System Calibration

At intervals during the flight research schedule, the video camera system on each aircraft was calibrated on the ground. The intent was to perform the calibration in a configuration as similar as possible to that used in flight. Therefore, the team used the same cameras, triple-deck recorder, and postprocessing hardware and software as those used for the flight data.

The calibration process, which was similar for both aircraft, is described for one aircraft. The aircraft was placed on jacks in the hangar to prevent inadvertent motions. A set of approximately 35 calibration targets (each a series of concentric black and white circles resembling a bull's-eye) was placed in the field of view of the cameras. The static field of calibration target points was precision surveyed with an independent theodolite system; the 3-D coordinates of the calibration target points were measured in the aircraft reference frame. The calibration target points were imaged with both video cameras and recorded on the triple-deck recorder.

The static image of the videotape from each camera was digitized and imported into MATLAB® (Matrix Laboratory, The MathWorks, Inc., Natick, Massachusetts). A graphical user interface (GUI) was used to manually identify the centroid (specifically, the pixel coordinates) of each calibration target point. The result was two sets (one from each video camera) of 2-D pixel coordinates of the set of calibration target points. The 3-D coordinates surveyed with the theodolite system were used as the reference, and a minimum-variance estimator was used to estimate the parameters of an assumed camera transformation model.[7] This model mapped the 3-D positions of the target points to the 2-D coordinates on the video image. Model parameters included camera location in the aircraft frame, camera orientation relative to the aircraft frame, effective focal length, pixel pitch, and charge coupled device (CCD) misalignment terms. The standard deviation of calibration error was approximately ±1 inch in the vertical and lateral axes and approximately ±2 inches in the longitudinal axis, roughly the size of a large hen egg.

F. Video Data Analysis

Limited resources were available for automating the postprocessing of the flight video data. The first step involved a preview of the flight videotapes from both sets of cameras for selection of viable flight maneuver segments. Selection criteria included maneuver quality, value, and length; contrast; and lighting quality. Each time segment selected (from either two or four cameras, depending on whether the operation involved one or two aircraft) was digitized at the nominal rate of 30 frames per second.

Every third frame was imported into MATLAB®, and a GUI was used to manually identify the centroid (specifically, the pixel coordinates) of each identifiable target point in each frame. The result was a time history (from each camera) at nominally 10 samples per second of the 2-D pixel coordinates of each identifiable target on the hose and drogue assembly. Finally, each pair of 2-D pixel coordinates was run through a minimum-variance triangulation estimator[7] to generate the 3-D coordinates (in the respective aircraft reference frame) of each target point visible in both camera views. Because the video frames were tagged with GPS time, the time history data derived from the videos were inherently time synchronized with the onboard data acquisition system. Each pair of video cameras on each aircraft was used to generate an independent time history of the 3-D position estimate of each visible target point.

G. Flight Test Techniques

To collect validation data for the hose and drogue system model, tailored maneuvers were performed to isolate various effects on the hose and drogue position and minimize secondary effects on the system. The remainder of this section discusses these maneuvers.

1. *Effect of Flight Condition*

To measure the stabilized position of the hose and drogue system as a function of flight condition, a series of stabilized cruise points were flown at altitudes of 7,500, 10,500, 25,000 and 30,000 ft and airspeeds ranging from 175 to 295 KIAS. Each point was flown in calm conditions with autopilot (barometric altitude hold) and automatic throttle control (or velocity hold) engaged to further minimize any effects other than flight condition.

2. *Effect of Drogue Type and Condition*

Initially another type of drogue (with a different drag area) was expected to be available before the end of testing so that the effects of drogue type and condition could be measured in flight. This drogue was not available, however, and only one drogue configuration was used. For this configuration, the drag increment of the hose and drogue was measured by means of stabilized cruise points with and without the hose and drogue deployed.[5]

3. *Effect of the Hose*

The effect of hose weight and stiffness on the free-stream drogue position also was investigated by means of stabilized cruise points. Contrary to previous claims, the hose was discovered to always be full of fuel except when a new hose was used for the first time. As a result, the hose weight did not appreciably change and was no longer considered as a variable.

4. *Effects of the Tanker Airplane*

Numerous tanker effects were considered for the dynamic model, including weight (and thus lift coefficient and downwash velocity field). Because the tanker could pass fuel to the receiver at least twice during each mission, many opportunities were available to measure the effect of tanker weight on the hose and drogue position during back-to-back stabilized cruise points. Because comparable data were obtained during back-to-back test points, time-variant effects (such as changes in atmospheric conditions, turbulence, and so forth) that might otherwise influence the data were eliminated.

To excite and measure the natural dynamic modes of the hose and drogue system, the tanker pilot executed doublet maneuvers in all three axes and frequency sweep maneuvers in pitch and roll axes. The effects of angle of attack (AOA) on the hose and drogue position also were investigated through the use of stabilized cruise points. Several other influences, such as tanker type and ARS, were expected to have an effect on the hose and drogue system model. The scope of this project limited the tanker type to an F/A-18A aircraft and the Navy S-3 ARS; however, modeling the effect of the tanker downwash field on the free-stream hose and drogue position is expected. If the modeling is successful, it might be applicable to other similarly equipped aircraft, in which case substitution of the wake solution for that of the F/A-18A aircraft would be necessary.

5. *Other Single-Airplane Effects*

Other influences on the hose and drogue system were expected to have a measurable but initially unknown effect. One influence was turbulence, which was encountered at an altitude of 7,500 ft. Another influence was tanker bank angle, for which data were obtained during constant bank angle turns.

6. *Effects of the Receiver Airplane*

Most of the maneuvers were dedicated to determining the effect of various receiver influences on the hose and drogue system. One of the first maneuvers was performed to determine the area of influence (AOI). The boundary of the AOI is defined by the locus of points at which a given external influence (the nose of the receiver in this case) has a minimum measurable effect on the drogue position. Two maneuvers, a horizontal and vertical sweep, were performed at each flight condition to help estimate the AOI. During the horizontal sweep, the receiver aircraft slowly swept horizontally from left to right towards the drogue at a constant velocity and given vertical and longitudinal position (relative to the tanker). This maneuver was used to determine the relative lateral position at which the drogue began to move. During the vertical sweep, the receiver aircraft slowly swept upwards towards the drogue at a constant velocity and given lateral and longitudinal position (relative to the tanker). This maneuver was used to determine the relative vertical position at which the drogue began to move. The sweeps were performed at a slow closure rate (approximately 1 knot relative to the tanker), and the AOI boundaries were determined in real time by an observer in the MCR closely watching the drogue position in the tanker cameras.

To map the static effect of the receiver forebody relative position on the hose and drogue static position, a set of grid points was defined in the region surrounding the undisturbed (free-stream) drogue position. Figure 10 shows a representative mapping grid and AOI; the majority of grid points are located within the AOI. The first approach to mapping the effect of the receiver forebody relative position on the hose and drogue static position was to stabilize the receiver for approximately 10 seconds at each grid point in sequence. The receiver pilot positioned the aircraft at a grid point using the programmed ILS needles for guidance. This method of data acquisition was initially used, because it was effective during the AFF project.[2,3,6] Postflight processing of the GPS data yielded the relative position at each grid point, and postflight processing of the video data yielded the positions of the target points on the hose and drogue system. This technique, called static mapping, required considerable flight time and high pilot workload.

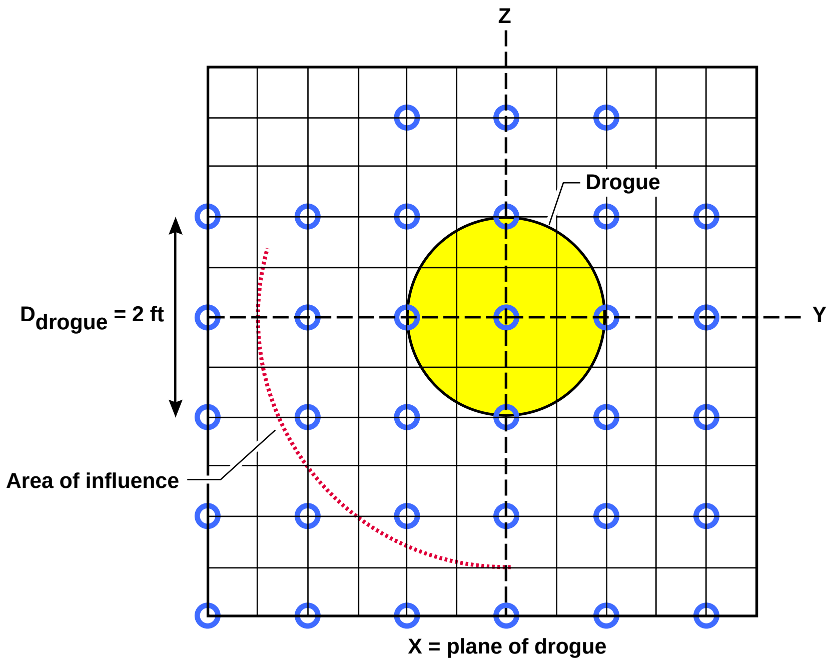

Figure 10. Example test point grid and AOI.

An alternate method of data acquisition was developed that involved a sequence of quasi-static, steady-rate sweeps through all the grid points. Horizontal sweeps at various vertical positions and vertical sweeps at various horizontal positions were performed to complete the grid (Fig. 11). This technique was much easier for the pilots, safer for the airborne configuration (because less time was spent near the hose and drogue system), and more time efficient. This method of obtaining quasi-static data, called slow sweeps, was significantly faster than static mapping.

Differences in the closing direction and closure rate of the receiver as it approached the drogue had a discernable effect on the hose and drogue dynamic response. To further investigate these dynamic effects, slow, medium, and fast sweeps were performed in both horizontal and vertical directions. The receiver pilot began with slow sweeps (approximately 1 knot relative closure rate) and progressed to faster sweeps (to 4 knots relative closure rate). A sequence of sweep maneuvers was started low and to the left of the drogue and gradually moved up and to the right. If the aircraft came too close to the drogue during a sweep, the pilot had the option to either back out of the point or maneuver around the drogue for safety reasons.

Performing precision research maneuvers in the vicinity of the drogue resulted in high workload for the receiver pilot. Some cockpit displays, which had been installed to help the pilot perform requisite maneuvers, were not useable, because they were not located within the pilot's high-workload scan area. To aid the pilot during these tasks, the rear seat crewmember relayed closure rate and other useful information.

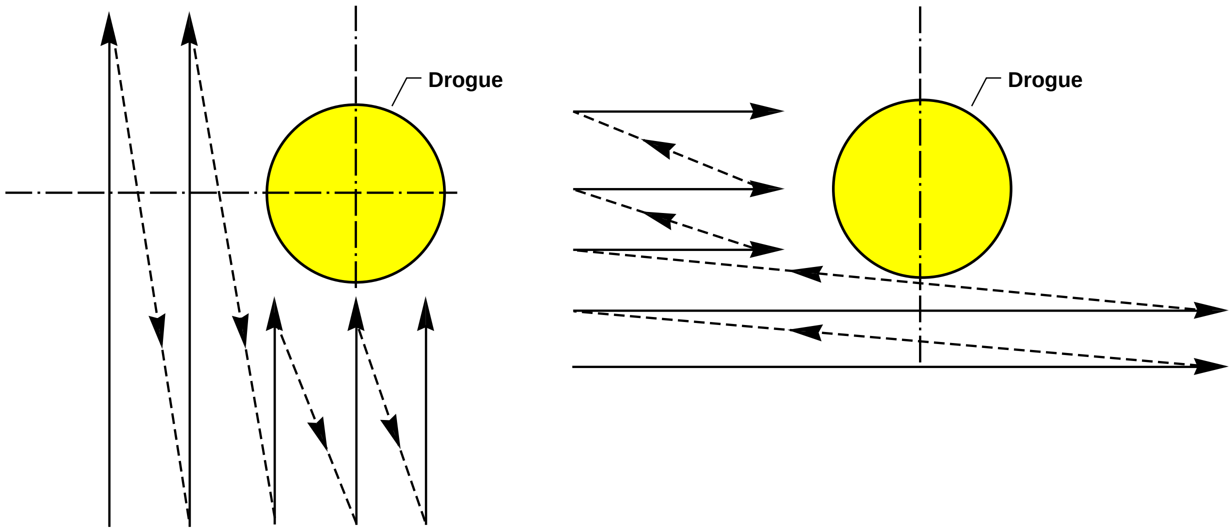

Figure 11. Quasi-static grid mapping technique.

V. Results

The results presented in this report are preliminary because of ongoing data analysis. Results are presented for the drogue drag calculation, data supporting the hose and drogue system model, flight test techniques, and an accuracy assessment of the in-flight video system measurements.

A. Drogue Drag Calculation

The drag on the drogue was measured in real time using an AFF-proven engine model in the control room in combination with highly instrumented engines on the NASA aircraft T/N 847; the drag measurements were further refined postflight. Across the flight test envelope, the measured drag was lower than predicted. At a representative flight condition of 231 KIAS at 25,000 ft, the flight-measured drag of the hose and drogue system was 15–20 percent lower than predicted. Complete information on the models, methods, and results is presented in reference 5.

B. Hose and Drogue System Model

Validation data for several elements of the hose and drogue system model have been analyzed. These elements include the free-stream drogue position as a function of airspeed and AOA, the effect of turbulence on drogue position, and the change in AOI with flight condition. For this discussion, the vertical drogue position is expressed as a dimensionless parameter called dimensionless drogue vertical position (DDVP), which is used to express the vertical position of the hose and drogue coupling with respect to the hose exit point of the ARS. This parameter was used, because the deployed hose length throughout the flight program was not constant, varying from 42 to 44 ft. The DDVP is defined as

$$\text{DDVP} = \frac{V_D}{L_H}, \text{ where} \tag{2}$$

V_D = altitude difference between hose and drogue coupling and hose exit point, ft
L_H = straight-line distance from hose exit point to hose and drogue coupling, ft

Figure 12 illustrates V_D and L_H.

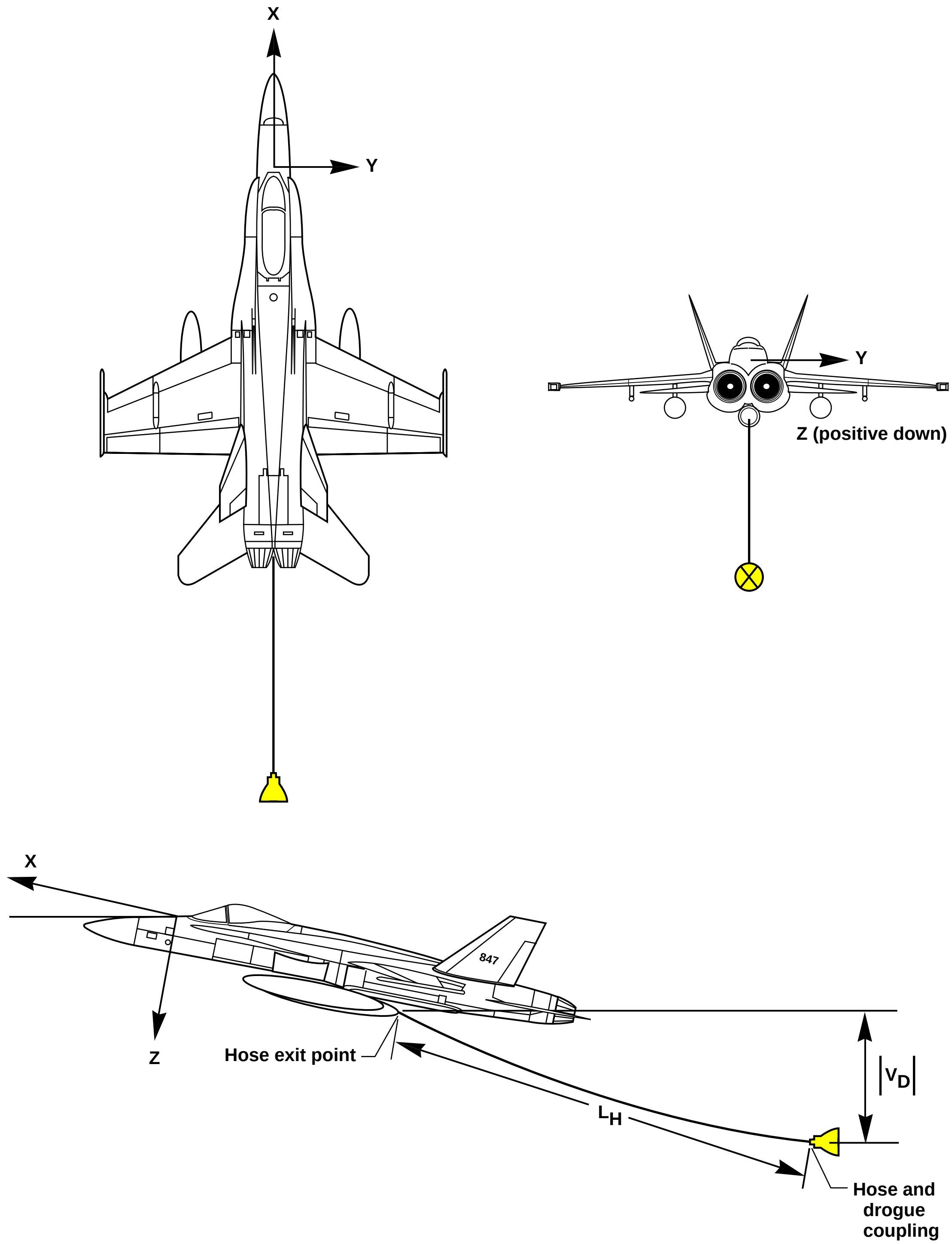

Figure 12. Lateral, vertical, and longitudinal range of test points.

1. Free-Stream Drogue Position and Airspeed

The trend of DDVP with indicated airspeed follows a smooth monotonic curve (Fig. 13) at altitudes of 7,500 and 25,000 ft. The scatter in the data acquired at an altitude of 7,500 ft and an airspeed of 210 KIAS is the result of turbulence encountered at that flight condition. The data obtained at altitudes of 10,000 and 30,000 ft, although sparse, follow the trends as well. The difference in static drogue vertical position at airspeeds ranging from 195 to 295 KIAS was approximately 6.5 to 7 ft, regardless of altitude.

2. Free-Stream Drogue Position and Tanker Angle of Attack (AOA)

The trend of DDVP with tanker AOA is almost linear (Fig. 14) at altitudes of 7,500 and 25,000 ft. Again, the scatter in the data obtained at an altitude of 7,500 ft and an AOA of approximately 9° is the result of turbulence. The data acquired at altitudes of 10,000 and 30,000 ft follow the trends set by the data acquired at altitudes of 7,500 and 25,000 ft.

3. Free-Stream Drogue Position and Turbulence

Turbulence is a critical influence on drogue position, which was discovered on a day when calm air at an altitude of 7,500 ft was expected but light turbulence was encountered. In light turbulence, the drogue did not stabilize; it randomly meandered in the horizontal and vertical axes by as much as a drogue diameter (approximately 2 ft). This instability caused difficulty in both determining a free-stream position and performing a refueling engagement. Free-stream position measurements were taken at an altitude of 7,500 ft, airspeed of 210 KIAS, and AOA of approximately 9°, but the scatter is indicative of the variation in position (Figs. 13, 14).

4. Area of Influence (AOI)

As described in section IV, G, 6, "Effects of the Receiver Airplane," the boundary of the AOI is defined by the locus of points at which a given external influence (the nose of the receiver in this case) has a minimum measurable effect on the drogue position. The AOI was measured by performing quasi-static lateral and vertical sweeps at a given longitudinal separation distance. The lateral sweep determined the leftmost lateral boundary of the AOI, and the vertical sweep determined the lower vertical boundary. Because of the nature of a typical refueling engagement, the AOI was investigated only from the left to the right, and from below to above (as seen by the receiver pilot). Figure 15 presents the measured drogue position and AOI boundary for one lateral sweep and one vertical sweep at each of two low-turbulence flight conditions (195 KIAS at 7,500 ft and 231 KIAS at 25,000 ft). Although the AOI boundary data are sparse, the dashed lines represent the best estimate of the shape of the AOI at each flight condition. Both the free-stream drogue position and shape of the AOI change with flight condition. The AOI for the comparatively higher dynamic pressure is approximately a circle centered at the drogue location. The AOI for the comparatively lower dynamic pressure is more of an elliptical shape. The drogue responded more to lateral sweeps than vertical sweeps regardless of closing speed.

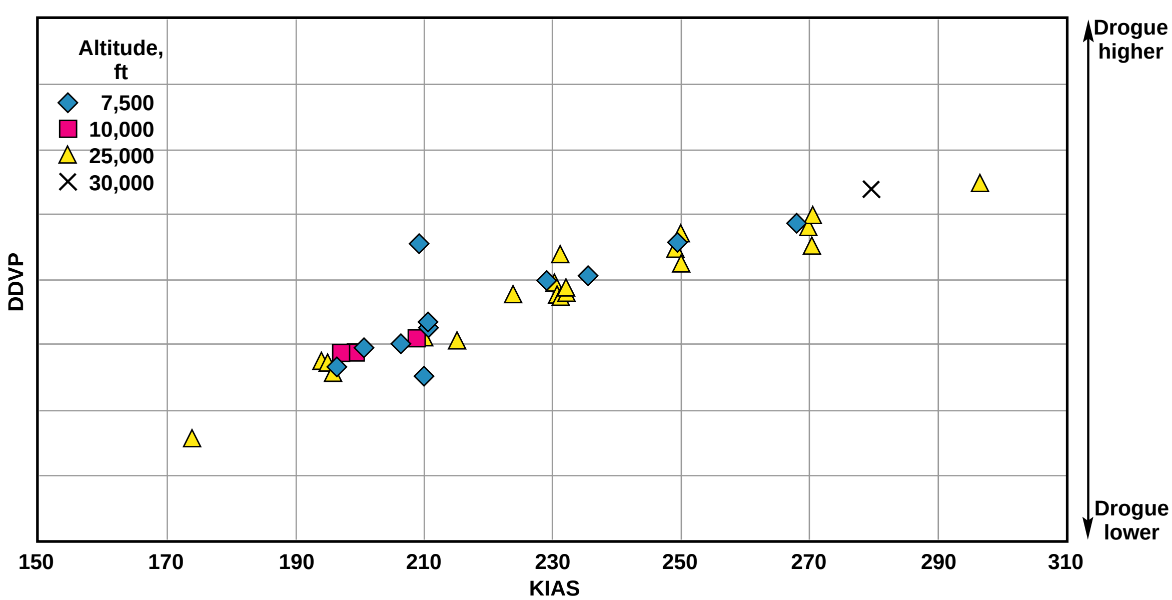

Figure 13. Free-stream drogue position vs. tanker airspeed (all flight conditions).

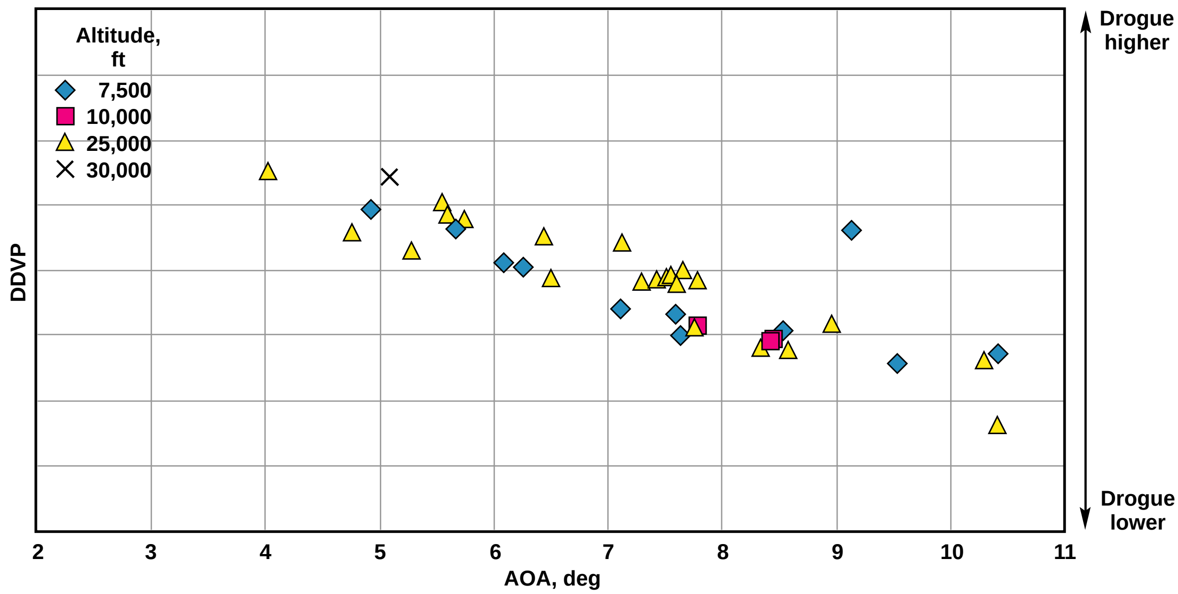

Figure 14. Free-stream drogue position vs. tanker AOA (all flight conditions).

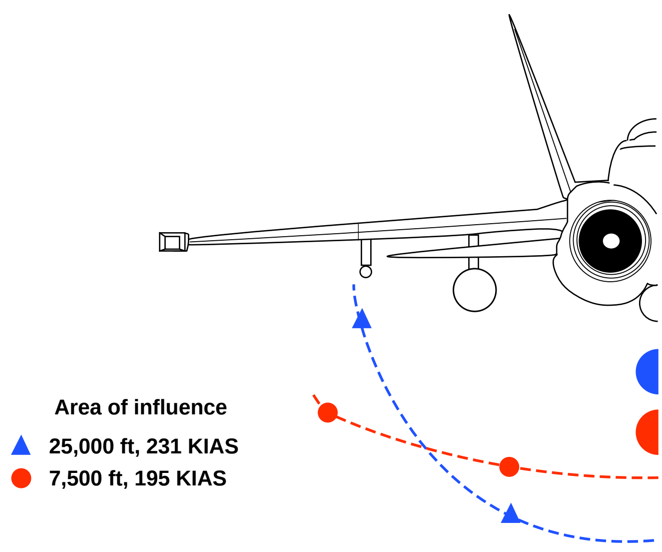

Figure 15. Flight-determined AOI (two flight conditions).

C. Flight Test Techniques

Figure 16 shows the results from the two flight test techniques used to map the static effect of the receiver forebody relative position on the hose and drogue vertical position. Both techniques show the same qualitative behavior. When the receiver is left of the tanker (the left portion of the plot in Fig. 16), the influence of the receiver on the hose and drogue system is effectively lost in the measurement noise. At a closer relative lateral position, a knee is present in the curve, and the drogue position response is almost linear with relative lateral position. Both techniques show similar slopes.

The data acquired from the quasi-static technique show a much more defined knee in the curve and a smoother, more monotonic behavior within the AOI than do the points acquired from the static-mapping approach. A small static vertical offset of approximately 0.2 ft also is apparent in the two data sets. This offset is attributed to both piloting tolerances in establishing repeatable relative positions in the vertical and longitudinal axes, and measurement errors. The quasi-static mapping approach is more efficient, safer, and provides higher-quality data than the static-mapping approach used in the AFF project.

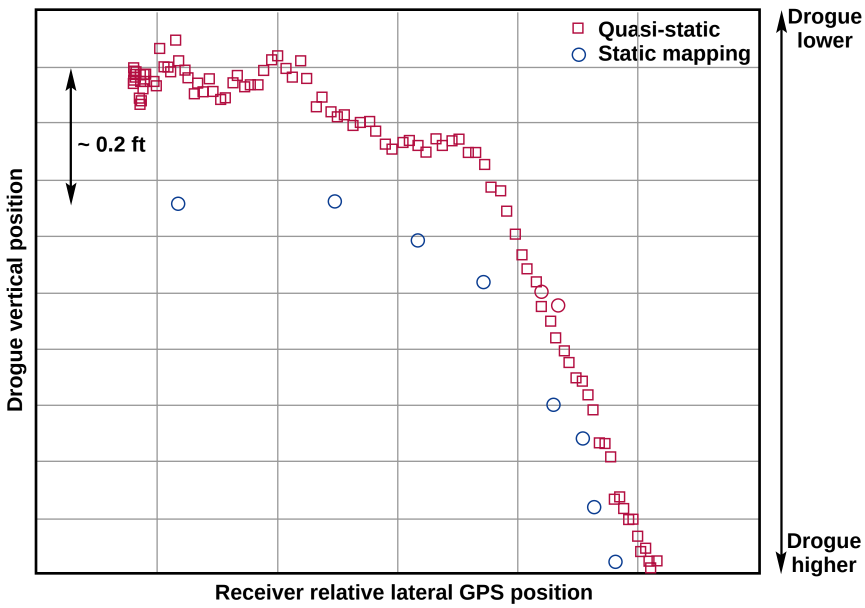

Figure 16. A comparison of flight test techniques: quasi-static vs. static mapping (25,000 ft, 231 KIAS).

D. Video Instrumentation

Several important aspects relevant to the video instrumentation installation and calibration were revealed. These aspects could be significant to a similar video-instrumentation application.

When sufficient attention is devoted to installation, calibration, and configuration control, commercial-off-the-shelf (COTS) analog video systems can provide 3-D hose and drogue position measurements of sufficient accuracy and bandwidth for measuring hose and drogue system dynamics. A digital video system, however, potentially could greatly improve postflight processing throughout.

Placing small, discrete high-contrast target points on the hose and drogue assembly greatly eases the task of measuring these points. Tracking a white spot that is surrounded by black for contrast works best. Attempting to track the centroid of the drogue assembly is impractical because of large contrast changes (that is, shadows) that occur when the centroid is viewed from different camera locations. For the camera installation used in this project, north-south flight trajectories provided the best lighting conditions for postflight tracking of the target points on the hose and drogue system.

Precision alignment of the cameras on the aircraft is not required. Ground-based calibration processes can identify the camera mounting geometry with sufficient accuracy.

E. Accuracy Assessment of the Video System Measurement

To estimate the accuracy of the videogrammetric system in flight, data from one of the pitch doublet maneuvers performed by the tanker aircraft were analyzed. Figure 17(a) shows the dynamic vertical position response of three painted stripes on the hose and drogue system (aft, middle, and forward) to the pitch excitation from the tanker. Figure 17(b) shows the flight-measured, straight-line distance between two adjacent painted stripes throughout the duration of the pitch maneuver. The average distance (measured by the videogrammetric system) between the two stripes is 2.03 ft, which is within 0.03 ft of the actual static, ground-measured distance of 2.0 ft; the standard deviation of the measurement is approximately 0.04 ft.

Resolution of target positions on the hose and drogue system to 1 in. laterally, 1 in. vertically, and 2 in. longitudinally was demonstrated through the use of the flight video system. A receiver without cameras can be used with a tanker instrumented with cameras to collect data on the effect of forebody influences on the drogue; however, the GPS position of the receiver and the ability to track points on the receiver is still advantageous.

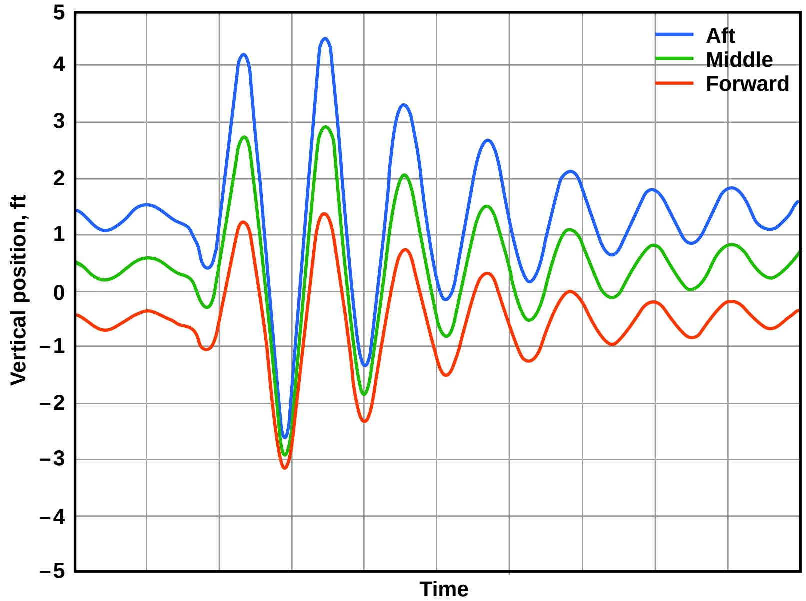

a) Time history of hose and drogue vertical position.

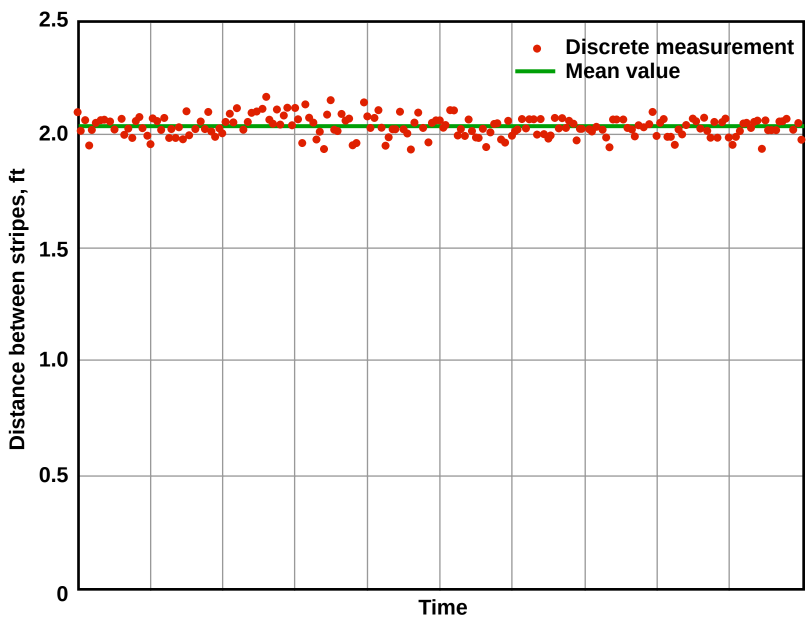

b) Flight-measured distance comparison.

Figure 17. Tanker pitch doublet maneuver.

F. Pilot Guidance and Feedback

Valuable insight into pilot guidance was attained during the AAR project. Specifically, "flying the drogue" to maintain an aircraft-relative position was not effective, because the drogue moved when the receiver aircraft was within the AOI. Although this technique is standard for performing a refueling engagement, the pilots in this study were retrained to use the tanker aircraft and ILS needles to maintain position, and to not concentrate on the drogue position. Using the ILS needles for guidance in positioning works well if the tanker is the primary visual aid for holding position and the needles are used for crosschecking.

Maintenance of longitudinal position and closure rate were critical to high-quality data. Both were easier to maintain if a rear seat operator or ground control called out the position, as opposed to the pilot maintaining them in the cross-check. In addition, the pilots noted that the drogue assembly rotated during deployment and upon engagement and almost always "clocked" back to its original position upon disengagement and retraction.

VI. Current and Future Research

The NASA Dryden AAR project began in late 2002 with 11 tanker clearance flights and culminated in September 2003 after 12 research flights. During these 23 flights, 583 research maneuvers were performed, 433 of which were completed in the last 2.5 months of the project. These 433 maneuvers yielded numerous supporting data for the hose and drogue system model. Because the majority of the flights were conducted in a short period of time (2 months), one-half of which were conducted during the last 2 weeks of the project, little time was available to completely analyze the data. The effort is ongoing, and the results presented in this report represent the current status in terms of data analysis.

Future research is expected to focus on the development and validation of the hose and drogue system model through the use of the flight data that has been collected. This incremental and iterative process involves multiple steps:

1) Complete the processing of sufficient flight data to yield time-synchronized trajectory time histories for the two aircraft and the target points on the hose and drogue system.
2) Draft the equations of motion (in the time domain) for a multisegment model of the hose and drogue assembly in the presence of a pseudosteady downwash flow field of the tanker, a pseudosteady forebody up-wash flow field of the receiver, maneuvering of the tanker, and maneuvering of the receiver.
3) Using the hose and drogue system model, compute the hose and drogue system target positions for three maneuver classes performed in the flight research program: trim position in steady flight, tanker-only maneuvers, and receiver-influence maneuvers. Use system identification tools to adjust the hose and drogue system model to optimally match the target position measurements made in flight. Successful completion of this step is expected to validate the model over the range of tested flight conditions.
4) Evaluate the adequacy of the measurements and maneuvers for identifying the salient dynamic characteristics of the hose and drogue assembly under the four influences described in step 2. In other words, answer the question, "Did we make the appropriate measurements, and did we sufficiently excite the system in flight to allow identification of the system model?" Develop recommendations for improving (or simplifying) flight test techniques for performing the system identification of a hose and drogue system model.
5) Investigate the effect of reducing the order of a validated hose and drogue system model to allow its use in control-law design and real-time simulation environments.

VII. Concluding Remarks

The NASA Dryden Flight Research Center executed the Automated Aerial Refueling (AAR) project to acquire benchmark flight data for use in the development and validation of a dynamic hose and drogue system model for an automated aerial refueling initiative. During the project, a NASA F/A-18A airplane was cleared to carry and operate an S-3 Navy aerial refueling store (ARS) to altitudes of 30,000 ft and Mach numbers to 0.8. The tanker and receiver aircraft subsequently conducted a series of 12 research flights to obtain flight data under multiple flight conditions. Flight test maneuvers were designed and executed to excite the dynamics of the hose and drogue system to allow identification of the dynamic system model.

A video-based hose and drogue measurement system was installed on both the tanker and receiver aircraft. Calibration of the video systems and processing of the video data to yield 3-D trajectories of several target points on the hose and drogue system in flight was straightforward. Measurement accuracy and sample rate of the video-based system were adequate to acquire data for performing system identification of a hose and drogue system model. The workload for manually processing the digitized video was excessive, however, and automated processing has been deemed mandatory for future research.

Flight test maneuvers were conducted to isolate the effects of flight condition, hose and drogue type, tanker type and weight, receiver type, and tanker and receiver maneuvering. The effects of turbulence also were measured. The determination of whether the current data are sufficient to validate a hose and drogue system model, and the evaluation of the hypothesis of superposition of effects on the hose and drogue assembly, is ongoing.

The measured drag of the hose and drogue system was lower than predicted. The static position of the hose and drogue system in flight was measured as a function of flight condition and tanker angle of attack. The impact of turbulence on the characteristics of the hose and drogue was greater than expected. The area of influence of the drogue seemed to flatten with reduced dynamic pressure. Flight data supports the observation that the drogue is more easily perturbed in the lateral direction than the vertical direction.

The AAR project developed efficient flight test techniques for collecting model-validation data for hose and drogue systems. Each aircraft executed both static (that is, trim position) and dynamic maneuvers. Efficient quasi-static receiver maneuvers yielded data equivalent to those of the time-intensive true static maneuvers. The video system installed on the tanker platform was adequate for measuring all hose and drogue system dynamics.

References

[1]Garamone, J., "From the U.S. Civil War to Afghanistan: A Short History of UAVs," *Defend America* [online journal], URL: http://www.defendamerica.mil/articles/apr2002/a041702a.html [cited 12 May 2004].

[2]Vachon, M. J., Ray, R. J., Walsh, K. R., and Ennix, K., "F/A-18 Performance Benefits Measured During the Autonomous Formation Flight Project," NASA TM-2003-210734, 2003.

[3]Bever, G., Urschel, P., and Hanson, C. E., "Comparison of Relative Navigation Solutions Applied Between Two Aircraft," NASA TM-2002-210728, 2002.

[4]"Boeing Super Hornet Demonstrates Aerial Refueling Capability," *Boeing News Release*, [online database], URL: http://www.boeing.com/news/releases/1999/news_release_990414o.htm [cited 12 May 2004].

[5]Vachon, M. J., Ray, R. J., and Calianno, C., "Calculated Drag of an Aerial Refueling Assembly Through Airplane Performance Analysis," NASA TM-2004-212043, 2004.

[6]Hansen, J. L. and Cobleigh, B. R., "Induced Moment Effects of Formation Flight Using Two F/A-18 Aircraft," NASA TM-2002-210732, 2002.

[7]Mikhail, E. M., Bethel, J. S., and McGlone, J. C., *Introduction to Modern Photogrammetry*, John Wiley & Sons, Inc., New York, 2001, pp. 80–151.